Award Number: 06HQGR0062

Title: CALIBRATING PAGER ("PROMPT ASSESSMENT OF GLOBAL EARTHQUAKES FOR RESPONSE") GROUND SHAKING AND HUMAN IMPACT ESTIMATION USING WORLDWIDE EARTHQUAKE DATASETS: COLLABORATIVE RESEARCH WITH USGS AND THE SWISS SEISMOLOGICAL SERVICE

Georgia Cua
Swiss Seismological Service, ETH Zürich
Schafmattstrasse 30
CH-8093, Zürich
Switzerland

Telephone: +41 44 633 7574
Fax: +41 44 633 1065
Email: georgia.cua@sed.ethz.ch

Title: *Calibrating PAGER ("Prompt Assessment of Global Earthquakes for Response") ground shaking and human impact estimation using worldwide earthquake datasets: collaborative research with USGS and the Swiss Seismological Service*

(Award number: 06HQGR0062)

Authors: G. Cua, D. Wald

Abstract

ShakeMaps are computer-generated maps that provide estimates of the geographical distribution of ground shaking in the minutes after an earthquake. ShakeMap ground shaking and intensity estimates are constrained by earthquake source information, observed peak ground motions, and ground motion prediction equations. Following a significant earthquake, the public can contribute felt reports over the internet using the "Did You Feel It" page. These felt reports are processed and used to generate Community Internet Intensity Maps. It is of interest to use observed intensities to constrain ground motion estimates in ShakeMap. This is useful in estimating peak ground motion distributions from historical earthquakes without instrumental observations, as well as generating ShakeMap ground motion and intensity estimates consistent with the Community Internet Intensity Maps. We explore the Bayesian approach proposed by Ebel and Wald (2003) to use both observed intensities and ground motion prediction equations to estimate peak ground motions on observed intensity and strong motion datasets from the 1994 M6.4 Northridge, California, 1998 M7.6 Kocaeli, Turkey, and 2005 M6.5 Bam, Iran earthquakes. We find that the performance of the Ebel and Wald (2003) approach depends heavily on the applicability of the ground motion to intensity relationships and ground motion prediction relationships for a given region. We propose a weighted-average approach for incorporating various types of data (observed peak ground motions, observed intensities, and predictions from ground motion prediction equations) into the ShakeMap ground motion and intensity estimation framework.

Introduction

The objective of the study is to determine how observations of modified Mercalli intensity (MMI) might be used to constrain peak ground shaking estimates (peak ground acceleration, peak ground velocity, and 5% damped response spectral acceleration values) in the aftermath of a significant earthquake. This is in large part motivated by the positive response of the public to Community Internet Intensity Maps (CIIM) and "Did You Feel It?" projects, which allow the public to report their experiences of earthquake ground shaking, and estimate the macroseismic intensity field after an earthquake based on these reports. The motivation for this study is to incorporate "Did You Feel It?" reports and other observations of modified Mercalli intensity into the ShakeMap system, thus producing a ground shaking estimates that are constrained by all available data: the observed peak ground motions at sites where seismic stations are installed, and the observed MMI and estimates from ground motion prediction equations elsewhere. Ebel and Wald (2003) had developed a probabilistic method for using observed MMI to constrain ground shaking estimates from past earthquakes; we use their Bayesian approach as a starting point.

Methodology

Ebel and Wald (2003) developed a Bayesian approach to estimating ground motions by combining contributions of from attenuation relationships and observed intensities. It is worthwhile to recap Bayes' theorem here for the reader to better understand Ebel and Wald (2003) approach. The following summary of Bayes' theorem is adapted from Sivia (1996), who provides an accessible and understandable presentation of Bayes' theorem and its applications.

Bayes' theorem states that

$$prob(hypothesis \mid data) = K \times prob(data \mid hypothesis) \times prob(hypothesis) \quad (1)$$

Each of these terms are probability density functions (pdf). *prob(hypothesis | data),* the left hand term, is known as the posterior distribution. The most probably hypothesis given the data is that which maximizes the posterior pdf. *prob(data|hypothesis)* is the likelihood function, and expresses the probability of observing the data, given that hypothesis is true. The likelihood function is how the data enters the estimation process in a Bayesian approach. *prob(hypothesis)* is known as the prior distribution; it expresses our belief in the hypothesis before we consider the data. *K* is a normalizing constant that ensures that *prob(hypothesis|data)* integrates to 1.

If we replace *hypothesis* and *data* in Eqn(1) with the corresponding quantities in our ground motion estimation application (namely, ground motion estimate (*GM*) and observed intensity (*MMI*), we get

$$prob(GM \mid MMI) \propto prob(MMI \mid GM) \times prob(GM) \quad (2)$$

The value of *GM* that maximizes *prob(GM|MMI)* is the most probable ground motion estimate. The spread of *prob(GM|MMI)* characterizes the uncertainty of this ground motion estimate. *prob(MMI|GM)* describes the probability of observing a given *MMI* level given a certain value of *GM*. Ebel and Wald (2003) describe how to derive *prob(MMI|GM)* using empirical relationships between peak ground motion parameters and *MMI* derived by Wald et al (1999b) using a California dataset.

Datasets

We applied the Bayesian estimation approach formulated by Ebel and Wald (2003) to observed ground motion and MMI datasets from the 1994 M6.5 Northridge, 1998 M7.6 Koaceli, Turkey, and 2003 M6.6 Bam, Iran earthquakes. The approach requires observed peak ground motion values used by ShakeMap (Wald et al., 1999a): peak ground acceleration (PGA), peak ground velocity (PGV), and 5% damped spectral acceleration at 0.3, 1.0, and 3.0 second periods (PSA0.3, PSA1.0, PSA3.0), as well as nearby located MMI observations.

Strong motion data

For the Northridge and Koaceli events, values for peak ground acceleration (PGA), peak ground velocity (PGV), and 5% damped spectral acceleration at 0.3, 1.0, and 3.0 second periods (PSA0.3, PSA1.0, PSA3.0) were obtained from the Next Generation Attenuation (NGA) project flatfile (Power et al., 2008). Strong motion data from Bam was not included in the NGA dataset. We downloaded acceleration time histories from the Iran Strong Motion Network (http://www.bhrc.gov.ir/ISMN/index.htm), and performed integration and filtering operations using SAC (Seismic Analysis Code).

Observed MMI

There was considerable variation in the quality of the MMI observations across the different earthquake datasets.

The MMI dataset for the Northridge event originally compiled by J. Dewey of the USGS (pers. comm.) and obtained for this study from David Wald. This dataset consisted of MMI assignment, latitude and longitude, postal code, and location string. Distances between the MMI locations and accelerometer station locations were calculated, and MMI value at the closest MMI observation was assigned to the station. The distances between MMI observations and accelerometer stations ranged from 0.26 to 2.98 km. There were 87 station-MMI observation pairs for the Northridge event.

No direct intensity observation points were available for the Kocaeli event. The MMI values were obtained by looking at station locations on an isoseismal map published by the Turkish Ministry of Public Work and Settlement (www.deprem.gov.tr). There were 22 station-MMI observation pairs for the Kocaeli event.

Intensity assignments at stations that recorded the Bam earthquake were made by Margaret Hopper, of the US Geological Survey's National Earthquake Information Center (NEIC). There were 12 station-MMI observation pairs for the Bam earthquake.

ShakeMaps

Purely predictive point source and finite fault ShakeMaps for the three events were provided by David Wald. These ShakeMaps were not constrained by observed ground motions, and thus were primarily controlled by the source characterization (point source or finite fault), the chosen attenuation relationship, and site amplification (as characterized by the average shear wave velocity in the upper 30 meters, Vs30). These predictive ShakeMaps were used to quantify the uncertainties in the predicted ground motions at a given site, due to having a point source or finite fault (Lin et al., 2005), as well as to provide Vs30 estimates at the seismic stations. The attenuation relationships used in this study accounted for site amplification using Vs30. Vs30 values were estimated at the stations by taking the Vs30 value at the closest ShakeMap grid point.

Analysis

We apply the Ebel and Wald (2003) approach to estimate the peak ground motion parameters from MMI observations from the 1994 M6.5 Northridge, 1998 M7.6 Kocaeli, and 2003 M6.5 Bam earthquakes. We used the Boore and Atkinson (2008) NGA relationship (BA2008) and the ShakeMap HazusPGV attenuation module (Wald et al., 2005). The ShakeMap HazusPGV module uses the Boore, Joyner, and Fumal (1997) relationship for PGA, and spectral quantities, and calculates PGV from 1.0-second PSA. These attenuation relationships predict peak ground motions as a function of magnitude, distance (epicentral distance for point source analyses, and Joyner-Boore distance for finite fault analyses), faulting style, and Vs30, and are used to generate the prior pdf *prob(GM)* in Eqn.(2). *prob(MMI|GM)* is derived by assuming that ground motions at a given MMI level are log-normally distributed with mean and standard deviations as listed in Table 1. Table 1 in this paper is identical to Table 3 from Ebel and Wald (2003). The dataset used by Ebel and Wald (2003) to derive the mean and standard deviations of various peak ground motion parameters at various MMI levels is identical to that used by Wald et al (1999b) in deriving the relationship between peak ground acceleration and peak ground velocity and MMI currently used by the ShakeMap codes. The peak ground motions are then estimated from the observed MMI using Eqn.(2). The estimated peak ground motions are then compared with the observed peak ground motion dataset.

We compare the performance of 3 types of ground motion prediction approaches (MMI only, attenuation only, Bayesian approach) using the Northridge, Kocaeli, and Bam strong motion / MMI datasets. Tables 2 through 4 list the root mean square (rms) error

$$\text{rms error} = \sqrt{\frac{\sum_{i=1}^{n} (\log Y_{pred,i} - \log Y_{obs,i})^2}{n}}$$

between the various ground motion predictions (Y_{pred}) and the available ground motion observations (Y_{obs}). (Throughout the paper, log refers to the natural log.) For each event, we perform point source and finite fault analyses using the BA2008 and HazusPGV relationships in turn. In each sub-table, the first row (*MMI only*) estimates peak ground motion using the relationship between mean ground motion level and MMI (Table 1). For instance, a PGA value of 43.3 cm/s/s with σ=0.86 would be estimated from an observed MMI level of IV. The second row predicts ground motion using an attenuation relationship (either BA2008 or HazusPGV). The third row predicts ground motion using the full Bayesian approach in Eqn.2, with *prob(GM)* defined by the attenuation relationship in the second row. The σ listed in Tables 2 through 4 are the uncertainties for the given attenuation relationship. For any given ground motion parameter (eg, PGA, PGV, etc), the values in **boldface** denote the prediction approaach with the lowest rms error. The highlighted values denote which of either attenuation only (BA2008/HazusPGV) or the full Baysian approach has the lower rms error.

1994 M6.5 Northridge, California

For the Northridge analysis, ground motions at 87 stations were estimated using the BA2008 and HazusPGV relationships (using reverse slip coefficients). Epicentral and Joyner-Boore distances (for finite fault analysis) of stations were obtained from the NGA flatfile. Uncertainties on the predicted ground motions were obtained from the respective point source and finite fault ShakeMap grid.xml files. Vs30 values at the 87 stations were also extracted from the ShakeMap grid.xml files and used to account for site amplification in BA2008 and HazusPGV ground motion predictions.

For both point source and finite fault analyses, all peak ground motion parameters, save 3.0 second PSA, are better fit by HazusPGV than by BA2008. Thus, the HazusPGV relationship is a better choice for defining *prob(GM)* than BA2008 (except for 3.0 PSA, where it would be better to use BA2008). In general, how well the Bayesian approach performs depends on how well the Ebel and Wald (2003) MMI-ground motion relationships fit the data. There are advantages in using the Bayesian approach over attenuation relationships alone if the relationship between MMI and ground motion is appropriate (in Table 1, when the rms error from MMI only is on the same order as that of the attenuation relationship only). The Bayesian approach will perform worse than the attenuation relationship if the relationship between MMI and ground motion does not fit the data well. This is the case with 0.3 second and 3.0 second PSA, where the rms value for MMI only are 2-3 times larger (with values of 1.15 and 1.59 respectively) than for the other ground motion parameters (with values on the order of 0.5). In such cases, it is better to use the attenuation relationship alone.

Figures 1 through 5 illustrate the performance of the various ground motion prediction approaches on the Northridge PGA, PGV, and 0.3-, 1.0-, and 3.0-second PSA datasets with point source and finite fault analyses. The uncertainties on the Ebel and Wald (2003) estimates (labeled "Bayes σ") are calculated by computing the cumulative density function of *prob(GM|MMI)* in Eqn.(2) and taking half the distance between the 16^{th} and 84^{th} percentiles. Note that the ShakeMap uncertainties for the point source cases exhibit a strong distance dependence due to the use of epicentral instead of fault distance (Lin et al., 2005). ShakeMap uncertainties for the finite fault cases (where fault distance is known) is a constant, as supplied by the attenuation relationship employed. The Bayes uncertainty is a function of the attenuation relationship and the ground motion to intensity relationship uncertainties, and it thus dependent on the observed MMI.

1998 M7.6 Kocaeli, Turkey

Table 3 lists the results from the Kocaeli strong motion-MMI dataset. Strike-slip coefficients were used to evaluate the BA2008 and HazusPGV relationships. For all cases considered (point source and finite fault analyses using BA2008 and HazusPGV), PGV is best predicted by the Wald (1999b) ground motion – MMI relationships alone. (In other words, the Kocaeli PGV dataset is not very well described by HazusPGV or BA2008.) In the finite fault analysis, the BA2008 relationship consistently fits the various ground motion parameters better than the HazusPGV relationship. As was observed with the Northridge dataset, the Bayesian approach performs better than the attenuation relationships alone when the rms of the MMI only predictions are on the same order as the rms error of the predictions from the attenuation relationships alone. For the Kocaeli dataset, such is the case for all ground motion parameters, save 3.0-second PSA when using the BA2008 attenuation relationship.

Figures 6 through 10 illustrate the performance of the various ground motion prediction approaches on the Kocaeli PGA, PGV, and 0.3-, 1.0-, and 3.0-second PSA datasets with point source and finite fault analyses.

2005 M6.5 Bam, Iran

Table 4 lists results from the Bam dataset (12 strong motion – MMI observation pairs). Interestingly, the point source modelling using BA2008 and HazusPGV fits the data better than the finite fault analysis. For all cases (similar to the Kocaeli dataset), PGV is best fit by the MMI only predictions. In general, neither BA2008 nor HazusPGV describe the observed ground motions well, with rms errors on the order of 1 or greater for all ground motion components. The Bayesian approach predicts the ground motions better than using an attenuation relationship alone. However, there are cases where the MMI only analysis performs better than the Bayesian approach.

Figures 11 through 15 illustrate the performance of the various ground motion prediction approaches on the Bam PGA, PGV, and 0.3-, 1.0-, and 3.0-second PSA datasets with point source and finite fault analyses.

Discussion and Conclusions

We compared the performance of 3 ground motion prediction approaches (the Wald (1999b) relationship between peak ground motion and MMI, the BA2006 and HazusPGV attenuation relationships, and the Bayesian approach of Ebel and Wald (2003) which combines the use of both MMI and attenuation relationships in estimating peak ground motion parameters) on joint strong motion-MMI datasets from the 1994 M6.5

Northridge, California, the 1998 M7.6 Kocaeli, Turkey, and the 2005 M6.5 Bam, Iran earthquakes.

In general, the Ebel and Wald (2003) approach of combining the contributions of observed MMI and estimates from attenuation relationships in estimating ground motion parameters has advantages over using an attenuation relationship alone if the employed relationship between ground motion and MMI is appropriate for the given region and ground motion range. In this study, we focused on the Ebel and Wald (2003) relationships between ground motion and intensity (Table 1) in defining *prob(MMI|GM)*. Other possible alternatives for defining *prob(MMI|GM)* include relationships between peak ground motion parameters and MMI developed by Wald et al (1999b), Atkinson and Kaka (2007), and Atkinson and Sonley (2000). For PGA and PGV for the Northridge, Kocaeli, and Bam earthquakes, the Bayesian approach performs better than the attenuation relationships alone. For response spectral at 0.3-, 1.0-, and 3.0-second periods, there are cases (for instance, 0.3- and 3.0-second response spectra from the Northridge dataset) wherein the ground motion-MMI relationship is perhaps not appropriate (and thus the *MMI only* cases in Tables 2 through 4 have large rms values) that the attenuation relationships alone perform better than the Bayesian approach. Surprisingly, it is not uncommon for the *MMI only* cases to have the lowest rms values, as is the case for PGV estimates from the Kocaeli and Bam datasets. The estimates from the Bayesian approach are poor if the attenuation relationships do not fit the observed data adequately (possibly due to regional differences in attenuation or unaccounted site amplification effects). It is interesting that using the HazusPGV relationship often results in lower rms values than the BA2008 relationship, which was derived from a much larger dataset.

A weighted average approach would accomplish the same end as the Bayesian approach of Ebel and Wald (2003) (combining the contributions of MMI observations and attenuation relationships in the estimation of peak ground motion at a given site) with the advantages of 1) skipping the step of generating *prob(MMI| GM)* from *prob(GM | MMI)* and 2) providing an analytical solution for both the mean ground motion and its corresponding uncertainty which can be obtained with fewer calculations than the "brute force" multiplication of 2 Gaussian pdfs called for by the Ebel and Wald (2003) approach.

Taking the weighted average of n normally distributed variables with mean Y_i, standard deviation σ_i, and weights $w_i = \frac{1}{\sigma_i^2}$ results in a normally distributed variable with mean $\bar{Y}$ and standard deviation $\bar{\sigma}$ given by:

$$\bar{Y} = \frac{\sum_{i=1}^{n} \frac{Y_i}{\sigma_i^2}}{\sum_{i=1}^{n} \frac{1}{\sigma_i^2}} \qquad \bar{\sigma}^2 = \frac{1}{\sum_{i=1}^{n} \frac{1}{\sigma_i^2}} \tag{3}$$

Thus, the combined contributions of ground motion estimates from 1) an MMI observation at a given site and 2) an estimate from an attenuation relationship (both can be described by log-normal distributions) would result in a log-normally-distributed ground motion estimate with mean $\bar{Y}$ and standard deviation $\bar{\sigma}$ given by:

$$\begin{aligned}
\bar{Y} &= \frac{\dfrac{Y_{MMI}}{\sigma_{MMI}^2} + \dfrac{Y_{atten}}{\sigma_{atten}^2}}{\dfrac{1}{\sigma_{MMI}^2} + \dfrac{1}{\sigma_{GMPE}^2}} = \frac{Y_{MMI}\sigma_{atten}^2 + Y_{atten}\sigma_{MMI}^2}{\sigma_{MMI}^2 + \sigma_{atten}^2} \\
\bar{\sigma}^2 &= \frac{1}{\dfrac{1}{\sigma_{MMI}^2} + \dfrac{1}{\sigma_{atten}^2}} = \frac{\sigma_{MMI}^2\sigma_{atten}^2}{\sigma_{MMI}^2 + \sigma_{atten}^2}
\end{aligned} \tag{4}$$

where Y_{MMI} and σ_{MMI} are as listed in Table 1, and Y_{atten} is the ground motion level predicted by an attenuation relationship with standard deviation σ_{atten}. (Note, this is the exact case being considered with the Ebel and Wald (2003) Bayesian approach.)

Gerstenberger et al (2007) use scalar correction factors to adjust for different 1) source-to-site distances and 2) site conditions to estimate ground motions at a given site (site A)

based on observed ground motions from a "nearby" station:

$$\begin{aligned}
Y_{corr,siteA} &= Y_{obs} \times C_{dist} \times C_{site_amp} \\
C_{dist} &= \frac{Y_{atten,siteA}}{Y_{atten,obs}} \\
C_{site_amp} &= \frac{SAF_{siteA}}{SAF_{obs}}
\end{aligned} \tag{5}$$

where $Y_{corr,siteA}$ is the ground motion estimate at site A arrived at by scaling the "nearby" observed ground motion Y_{obs} by a distance correction term C_{dist} and a term accounting for differences in site amplification factor C_{site_amp}. In Eqn.(5) $Y_{atten,siteA}$ and $Y_{atten,obs}$ are ground motion estimates from an appropriate attenuation relationship at site A and the site of observed ground motion, respectively. SAF_{siteA} and SAF_{obs} are site amplification factors at site A and the site of observed ground motion, respectively. Gerstenberger el al (2007) found that $Y_{corr,siteA}$ is log-normally distributed, and currently describe $\sigma_{corr,siteA}$ as a constant (0.31 in southern California). They are currently investigating the dependence of $\sigma_{corr,siteA}$ on the following: 1) distance from event; 2) distance between sites A and observation; 3) earthquake magnitude; 4) observation - event - site A azimuth; and 5) hypocentral depth.

The weighted average approach in Eqn.(3) can be easily extended to a general case of interest in ShakeMap calculations – estimating ground motions at a site with "nearby" MMI observations, "nearby" peak ground motion observations, and ground motion estimates from an attenuation relationship by applying the scalar corrections in Eqn.(5).

In this case, the ground motion estimate would again be a log-normally-distributed variable with mean and standard deviations
given by:

$$\bar{Y} = \frac{\frac{Y_{atten}}{\sigma^2_{atten}} + \sum_{i=1}^{n} \frac{Y_{corr,MMI,i}}{\sigma^2_{corr,MMI,i}} + \sum_{j=1}^{m} \frac{Y_{corr,sta,j}}{\sigma^2_{corr,sta,j}}}{\frac{1}{\sigma^2_{atten}} + \sum_{i=1}^{n} \frac{1}{\sigma^2_{corr,MMI,i}} + \sum_{j=1}^{m} \frac{1}{\sigma^2_{corr,sta,j}}}$$

$$\bar{\sigma}^2 = \frac{1}{\frac{1}{\sigma^2_{atten}} + \sum_{i=1}^{n} \frac{1}{\sigma^2_{corr,MMI,i}} + \sum_{j=1}^{m} \frac{1}{\sigma^2_{corr,sta,j}}} \qquad (6)$$

In Eqn.(6), $Y_{corr,sta,j}$ and $\sigma_{corr,sta,j}$ are the ground motion and corresponding uncertainty estimates at the site of interest scaled as described by Gerstenberger et al (2007) and Eqn.(5) from "nearby" observed ground motions. $Y_{corr,MMI,j}$ and $\sigma_{corr,MMI,j}$ are the ground motion and uncertainty estimates at the same site scaled from "nearby" observed MMI. We can scale the ground motion estimate from the site of an MMI observation to another nearby site again using Eqn.(5), with Y_{obs} replaced by Y_{MMI} as listed in Table 1. Further investigation is required to quantify $\sigma_{corr,MMI}$. Setting $\sigma_{corr,MMI}$ equivalent to σ_{MMI} in Table 1 provides a reasonable lower bound for the uncertainty estimate for the contribution of this term. Possible criteria for "nearby" for observed ground motions would be "stations within 10 km of site of interest". A possible criteria for "nearby" observed MMI would be "MMI observations within 2 (or 3) km of site of interest".

A possible framework for combining different types of data consistently in the ShakeMap codes would thus be the following:

1) At locations with available ground motion observations, the ShakeMap output ground motion grids should reflect the observed values (this is the case with the existing ShakeMap codes)
2) At other locations, use Eqn.(6) to estimate the ground motions
3) At all locations, estimate intensity from ground motion estimates in Step 2 using standard ShakeMap processing
4) Replace estimated MMI with available observed MMI (and possibly smooth) for output MMI grid

Tables and Figures

Table 1: Mean and standard deviations of ground motion parameters at given MMI levels. (Table 3 in Ebel and Wald (2003), used to determine *prob(MMI | GM)* in Eqn.2. PGA and PSA are in units of cm/s/s, PGV in units of cm/s. The standard deviation σ is expressed in natural log units.)

MMI	PGA	σ	PGV	σ	PSA0.3	σ	PSA1.0	σ	PSA3.0	σ
IV	43.3	0.86	4.9	0.97	34.3	1.03	51.6	1.22	41.6	1.76
IV-V	65.2	0.83	5.4	0.83	56.1	0.92	69.5	1.04	43.0	1.42
V	68.9	0.81	6.0	0.82	60.0	0.89	72.4	1.01	43.2	1.36
V-VI	95.5	0.82	8.5	0.83	87.5	0.85	104.6	0.95	58.6	1.24
VI	130.4	0.70	11.2	0.64	125.4	0.64	148.6	0.73	78.4	1.01
VI-VII	159.4	0.67	16.0	0.64	150.2	0.66	208.6	0.76	123.1	1.02
VII	204.1	0.52	21.7	0.47	187.5	0.61	316.5	0.58	214.3	0.73
VII-VIII	240.4	0.61	25.5	0.55	219.5	0.68	364.2	0.67	225.8	0.83
VIII	459.5	0.46	40.8	0.60	409.2	0.58	633.8	0.71	277.6	1.15
VIII-IX	489.6	0.48	46.5	0.67	410.4	0.54	728.5	0.71	385.8	1.13
IX	563,2	0.50	82.9	0.45	413.0	0.47	989.6	0.64	796.2	0.67

Table 2: Ebel and Wald (2003) analysis on Northridge strong motion – MMI dataset

Point source using HazusPGV

	PGA (σ=0.52)	PGV (σ=0.558)	SA0.3 (σ=0.522)	SA1.0 (σ=0.633)	SA3.0 (σ=0.672)
MMI only	0.4727	0.4715	1.1523	0.5663	1.5930
HazPGV	0.4957	0.5931	**0.5032**	0.6229	**1.0237**
BayesHaz	**0.4138**	**0.4109**	0.6290	**0.4611**	1.0876

Point source using BA2006

	PGA (σ=0.5640)	PGV (σ=0.56)	SA0.3 (σ=0.6080)	SA1.0 (σ=0.6470)	SA3.0 (σ=0.6950)
MMI only	**0.4727**	0.4715	1.1523	0.5663	1.5930
BA06	0.6384	0.6684	**0.6603**	0.7035	0.7694
BayesBA06	0.5067	**0.4389**	0.8025	**0.4830**	**0.6893**

Finite fault using HazusPGV

	PGA (σ=0.52)	PGV (σ=0.558)	SA0.3 (σ=0.522)	SA1.0 (σ=0.633)	SA3.0 (σ=0.672)
MMI only	0.4727	0.4715	1.1523	0.5663	1.5930
HazPGV	0.4179	0.4258	**0.4321**	0.4265	**1.1081**
BayesHaz	**0.3786**	**0.3709**	0.4945	**0.4214**	1.1648

Finite fault using BA2006

	PGA (σ=0.5640)	PGV (σ=0.558)	SA0.3 (σ=0.522)	SA1.0 (σ=0.633)	SA3.0 (σ=0.672)
MMI only	0.4727	0.4715	1.1523	0.5663	1.5930
BA2006	0.4689	0.4322	**0.4858**	0.4747	**0.5714**
BayesBA06	**0.4429**	**0.3756**	0.65311	**0.4243**	0.6738

Table 3: Ebel and Wald (2003) analysis of the Kocaeli strong motion-MMI dataset

Point source HazusPGV

	PGA (σ=0.52)	PGV (σ=0.58)	SA0.3 (σ=0.522)	SA1.0 (σ=0.633)	SA3.0 (σ=0.672)
MMI only	0.6658	**0.4812**	**0.6625**	0.7962	1.2016
HazusPGV	0.6446	0.6577	0.7348	0.8407	0.8838
Bayes	**0.5617**	0.5291	0.6767	**0.7452**	**0.7789**

Point Source BA2006

	PGA (σ=0.5640)	PGV (σ=0.56)	SA0.3 (σ=0.6080)	SA1.0 (σ=0.6470)	SA3.0 (σ=0.6950)
MMI only	0.6658	**0.4812**	**0.6625**	0.7962	1.2016
BA2006	0.7202	0.6884	0.8699	0.9001	**0.5777**
Bayes	**0.5258**	0.5325	0.7507	**0.6835**	0.6370

Finite fault HazusPGV

	PGA (σ=0.52)	PGV (σ=0.58)	SA0.3 (σ=0.522)	SA1.0 (σ=0.633)	SA3.0 (σ=0.672)
MMI only	**0.6658**	**0.4812**	0.6625	**0.7962**	**1.2016**
HazusPGV	0.8242	0.7304	0.8047	1.1275	1.2964
Bayes	0.7461	0.5930	**0.6298**	0.9468	1.2424

Finite fault BA2006

	PGA (σ=0.5640)	PGV (σ=0.56)	SA0.3 (σ=0.6080)	SA1.0 (σ=0.6470)	SA3.0 (σ=0.6950)
MMI only	0.6658	**0.4812**	0.6625	0.7962	1.2016
BA2006	0.6748	0.5666	0.6466	0.8194	**0.6471**
Bayes	**0.6207**	0.4908	**0.5705**	**0.7690**	0.7907

Table 4: Ebel and Wald (2003) analysis of the Bam strong motion-MMI dataset

Point source using HazusPGV

	PGA (σ=0.52)	PGV (σ=0.558)	SA0.3 (σ=0.522)	SA1.0 (σ=0.633)	SA3.0 (σ=0.672)
MMI only	**0.9268**	**0.7460**	**0.7547**	**1.0083**	**1.5375**
HazPGV	1.1046	1.4490	1.0344	1.6642	2.0733
BayesHaz	0.9383	1.1019	0.7665	1.3469	1.8266

Point source using BA2006

	PGA (σ=0.5640)	PGV (σ=0.56)	SA0.3 (σ=0.6080)	SA1.0 (σ=0.6470)	SA3.0 (σ=0.6950)
MMI only	0.9268	**0.7460**	0.7547	**1.0083**	1.5375
BA06	0.7800	1.2856	1.0272	1.7816	1.5961
BayesBA06	**0.6419**	0.9771	**0.6899**	1.4161	**1.3710**

Finite fault using HazusPGV

	PGA (σ=0.52)	PGV (σ=0.558)	SA0.3 (σ=0.522)	SA1.0 (σ=0.633)	SA3.0 (σ=0.672)
MMI only	**0.9268**	**0.7450**	**0.7547**	**1.0083**	**1.5375**
HazPGV	1.1686	1.5422	1.1258	1.7583	2.1658
BayesHaz	0.9891	1.1697	0.8301	1.4147	1.9120

Finite fault using BA2006

	PGA (σ=0.5640)	PGV (σ=0.56)	SA0.3 (σ=0.6080)	SA1.0 (σ=0.6470)	SA3.0 (σ=0.6950)
MMI only	0.9268	**0.7460**	**0.7574**	**1.0083**	1.5375
BA06	0.9062	1.3777	1.1345	1.8740	1.6793
BayesBA06	**0.7477**	1.0506	0.7689	1.4986	**1.4528**

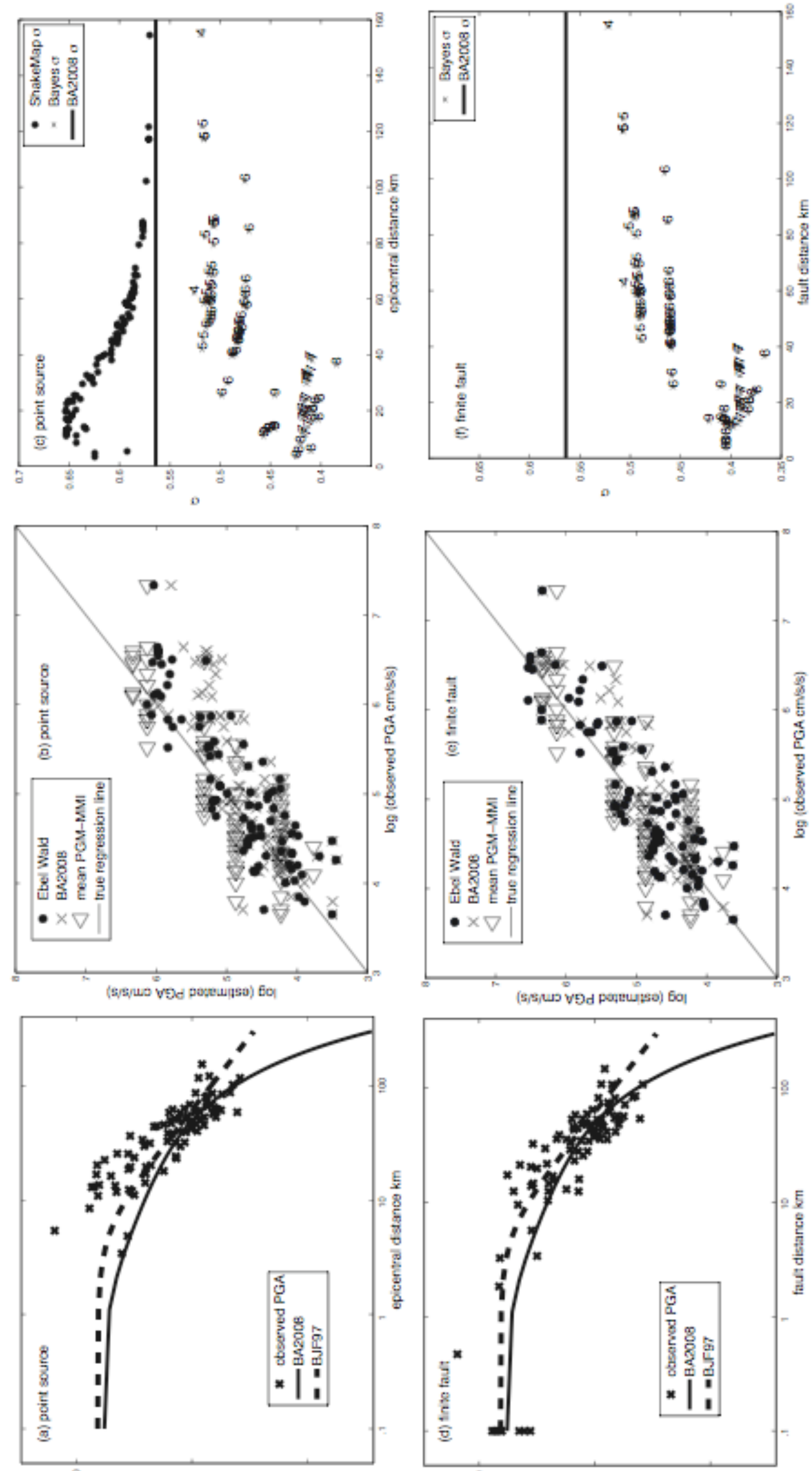

Figure 1: Northridge PGA

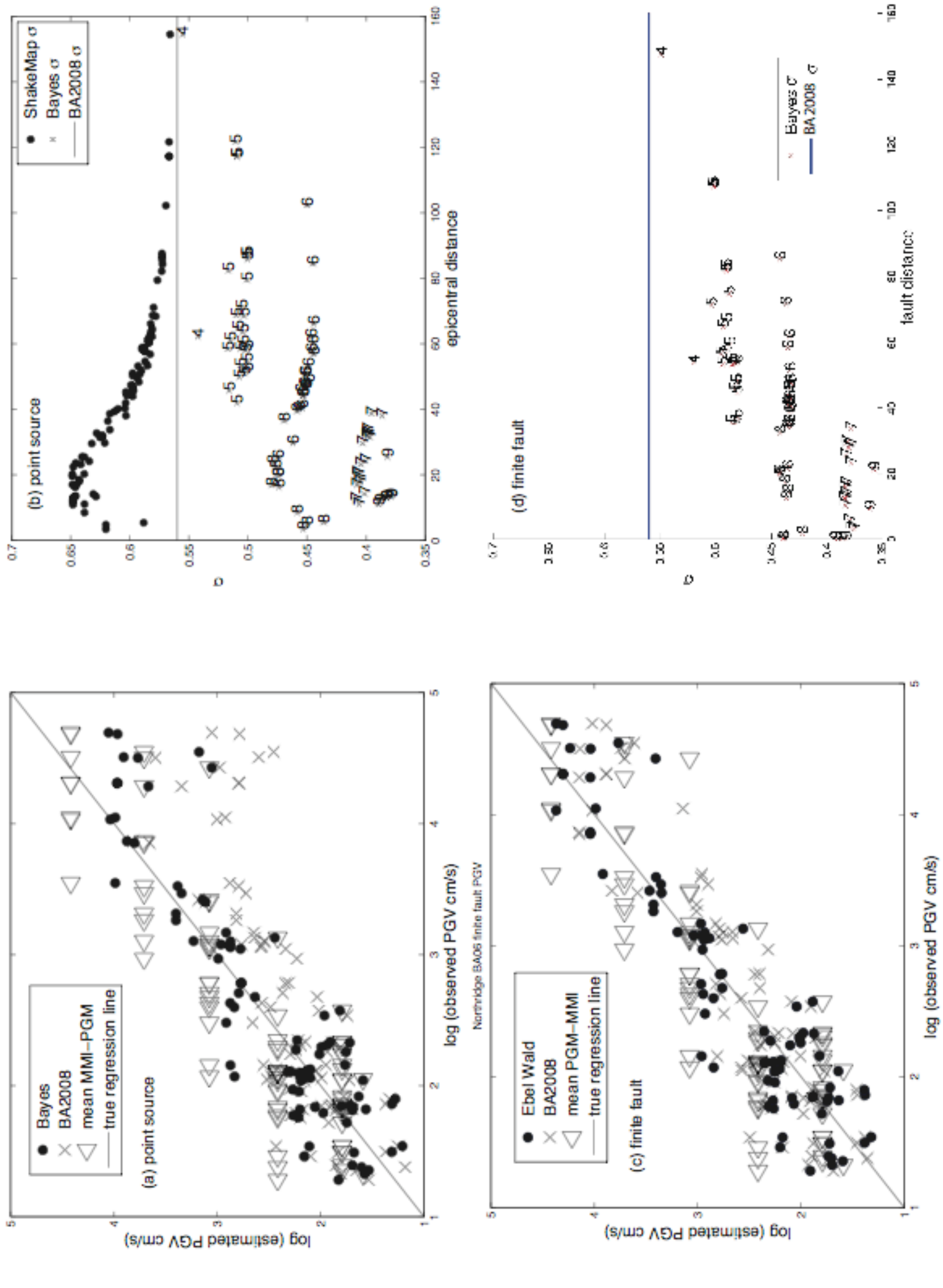

Figure 2: Northridge PGV

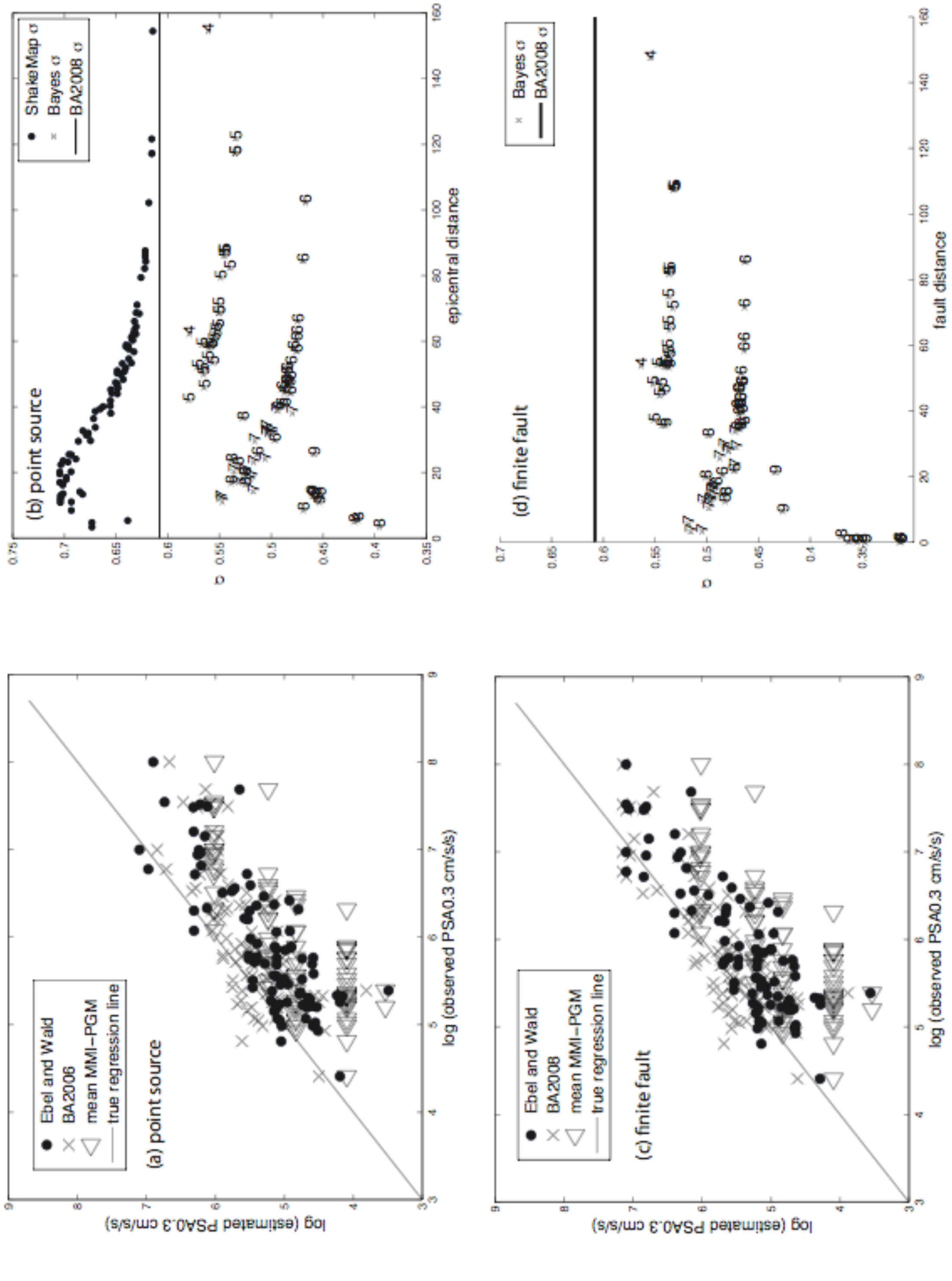

Figure 3: Northridge PSA 0.3 second period

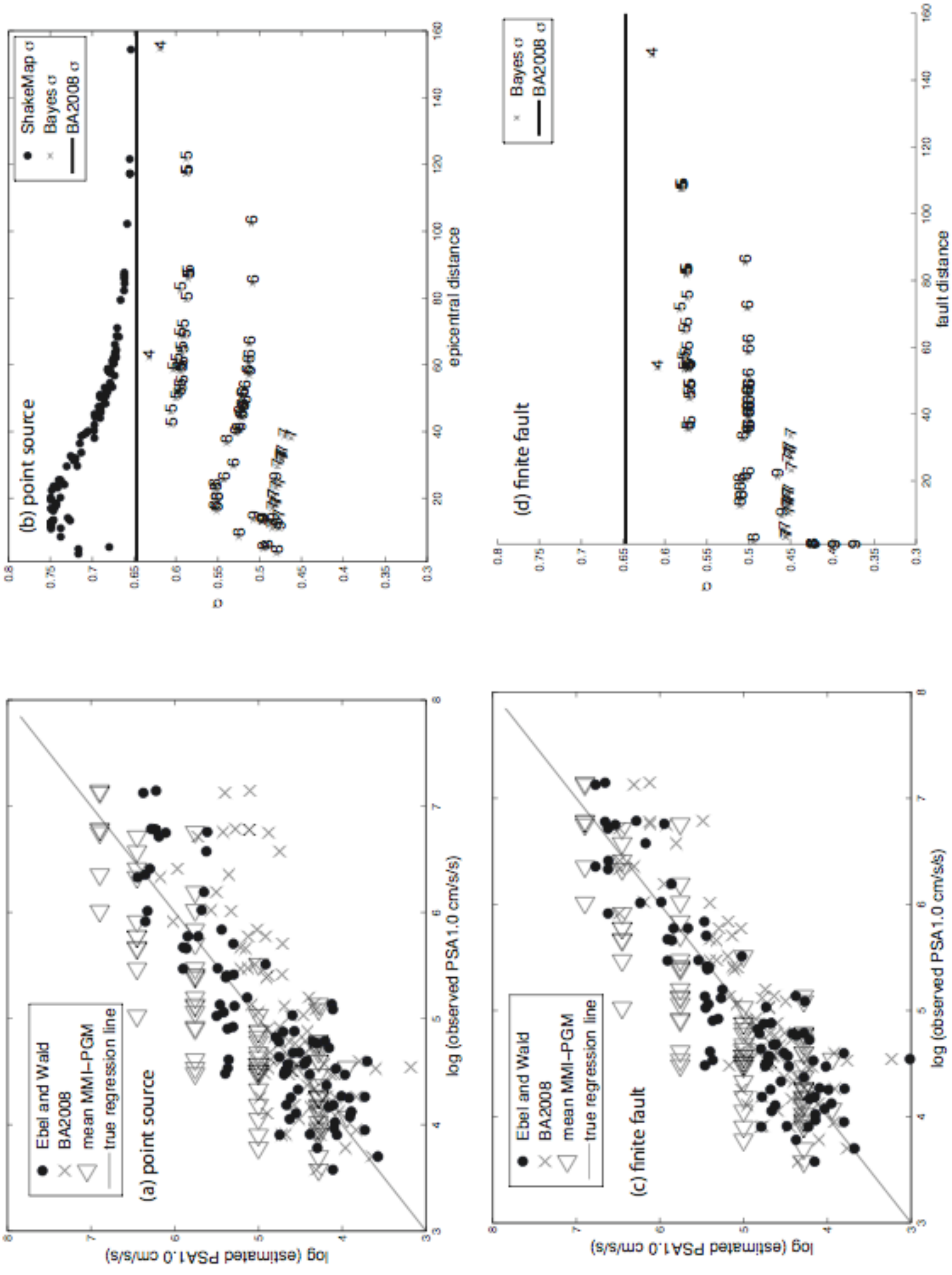

Figure 4: Northridge PSA 1.0 second period

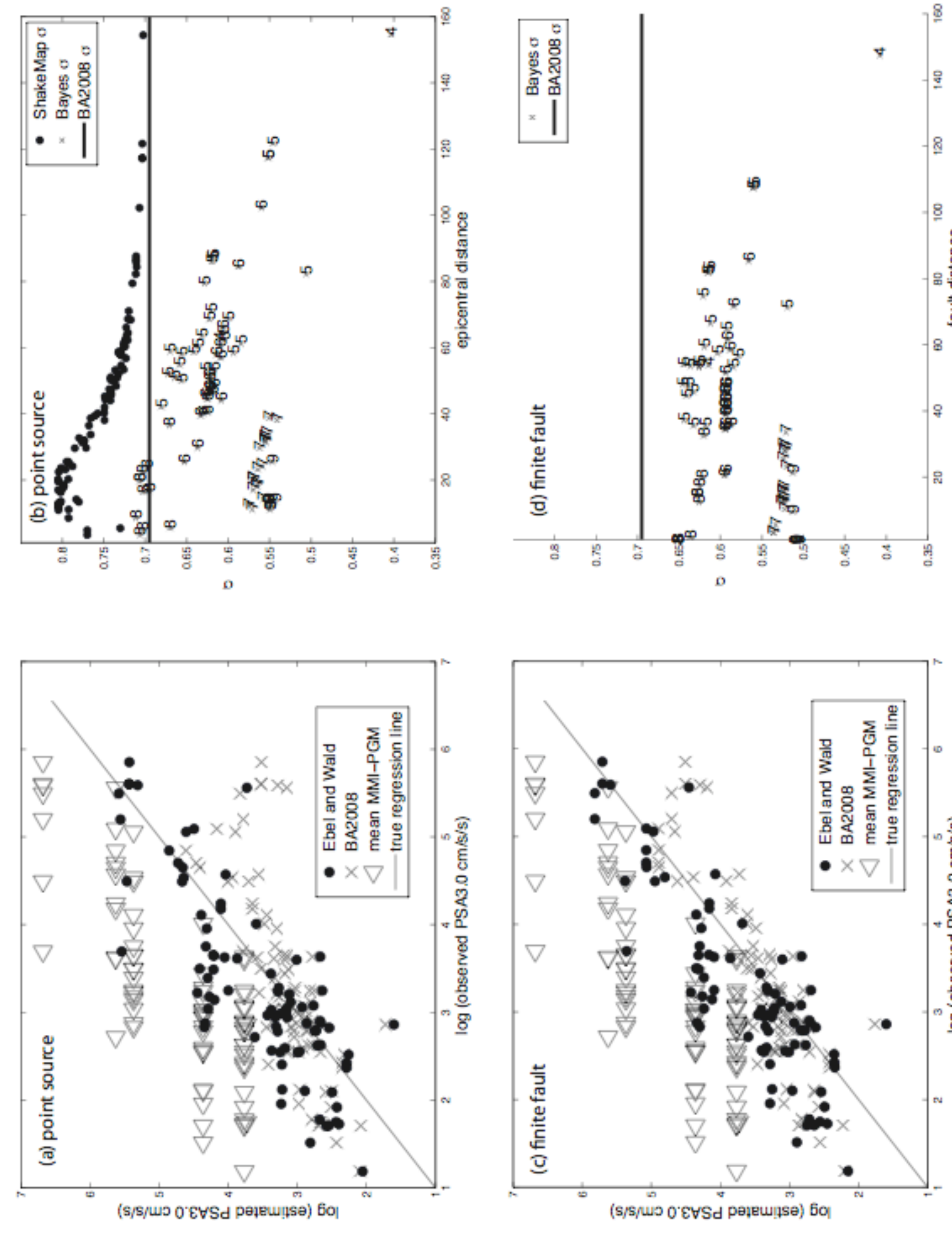

Figure 5: Northridge PSA 3.0 second period

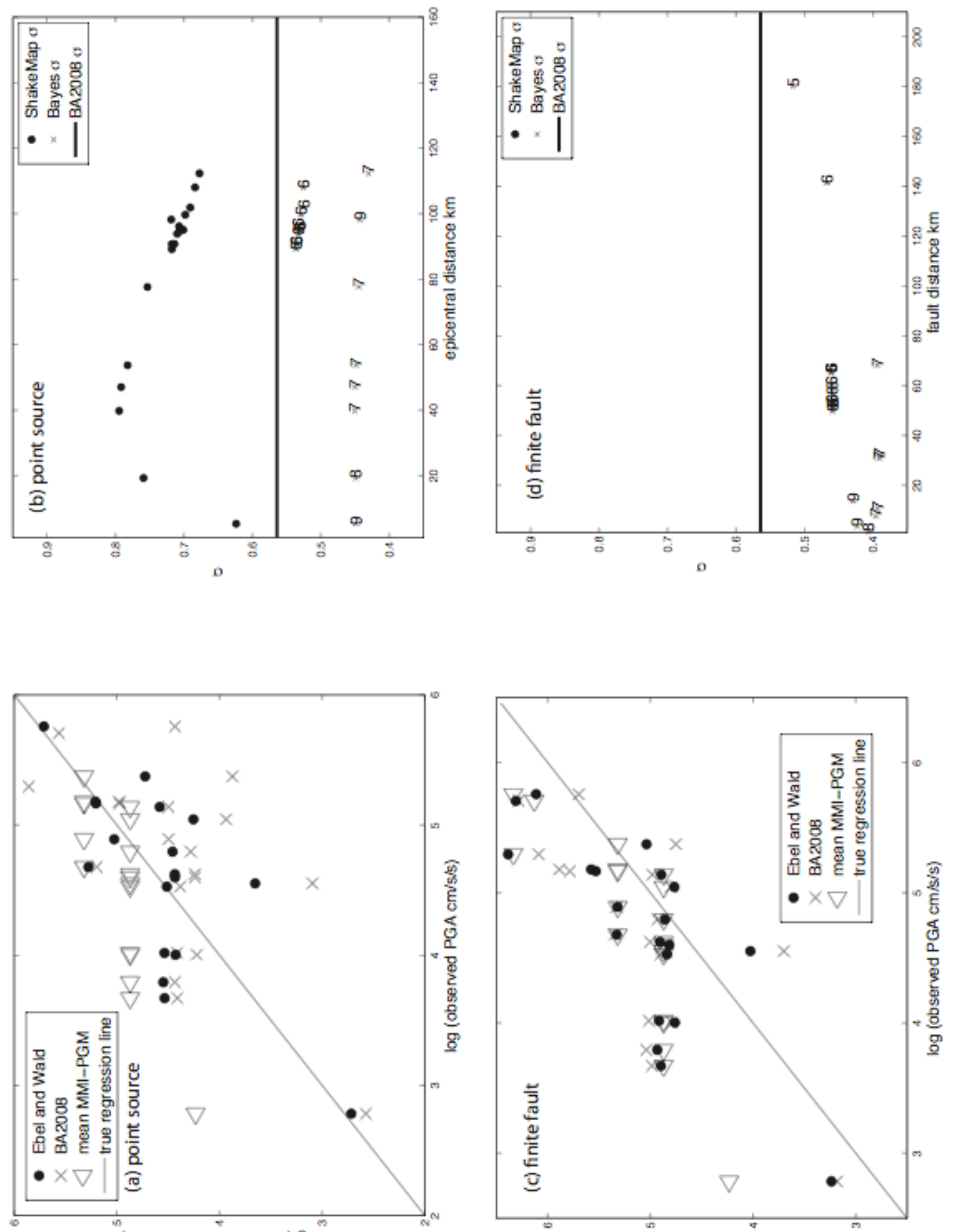

Figure 6: Kocaeli PGA

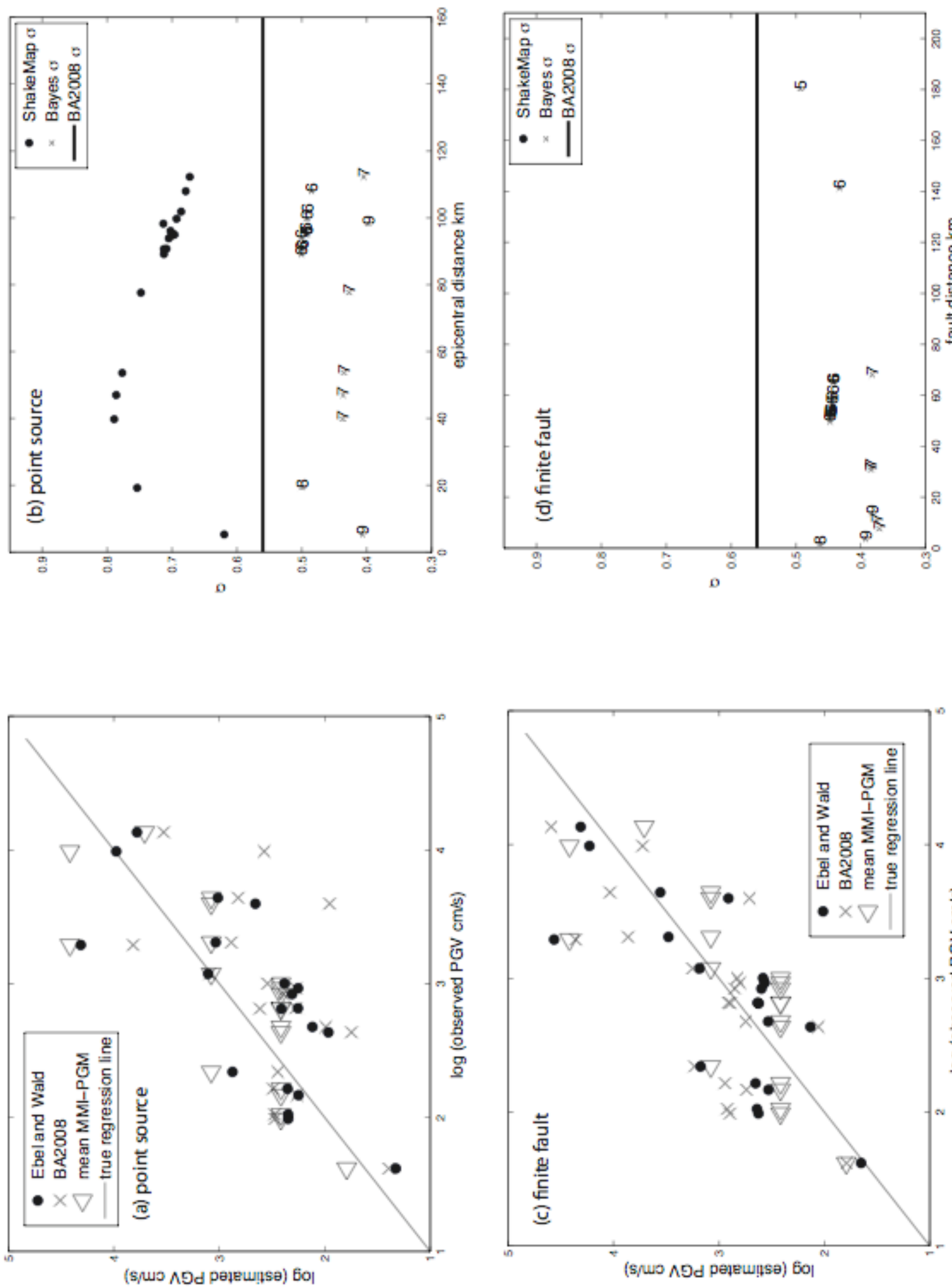

Figure 7: Kocaeli PGV

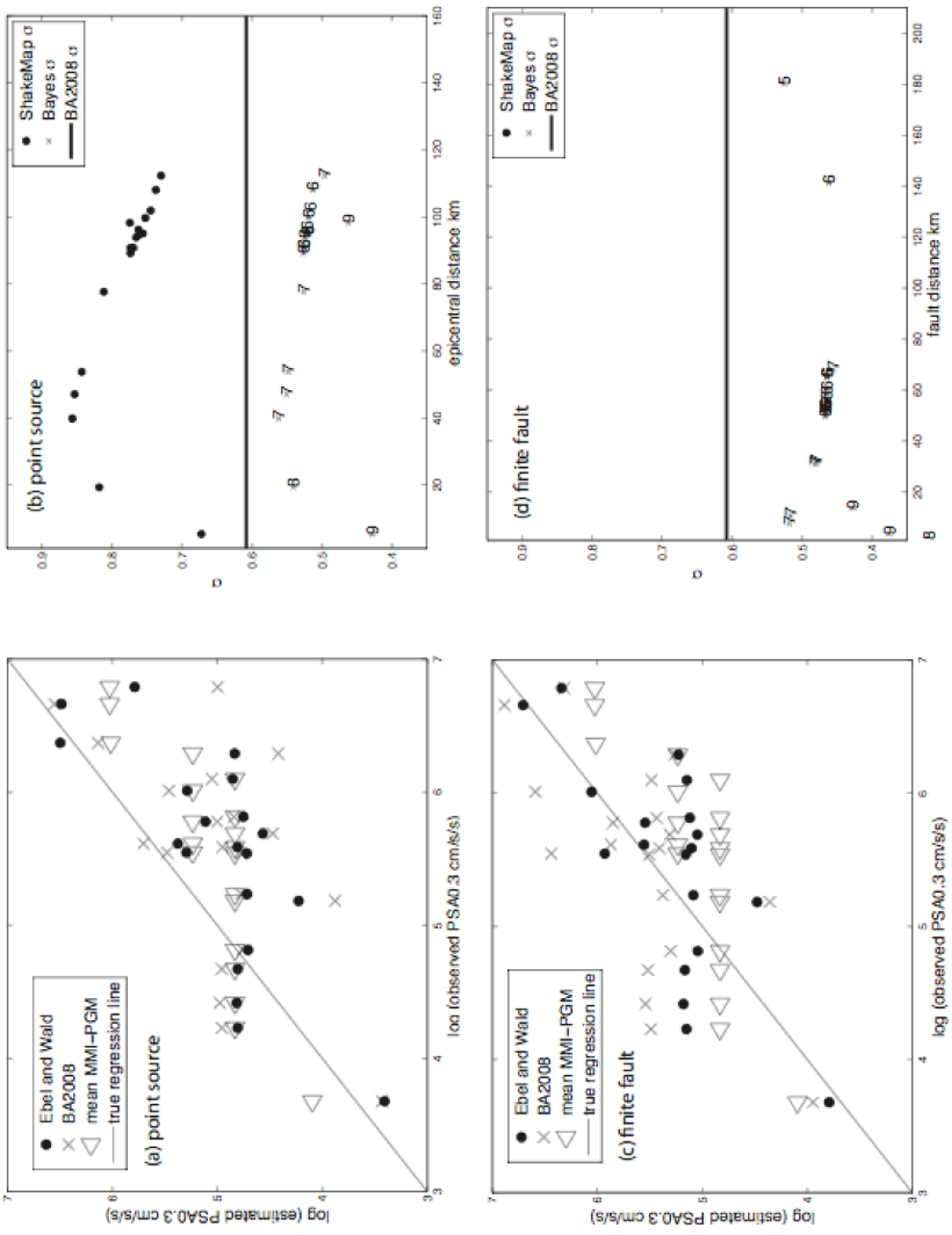

Figure 8: Kocaeli PSA 0.3 second period

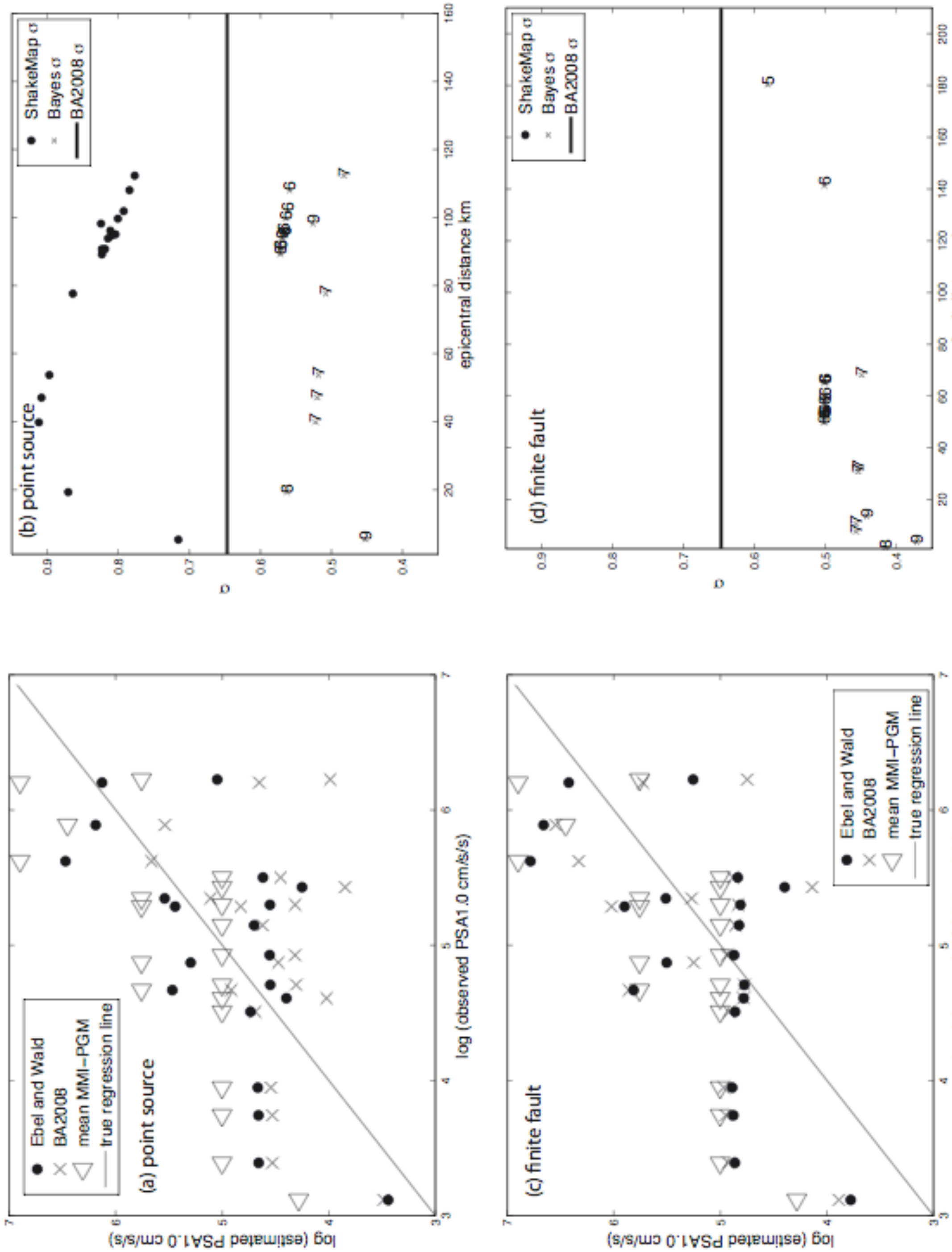

Figure 9: Kocaeli PSA 1.0 second period

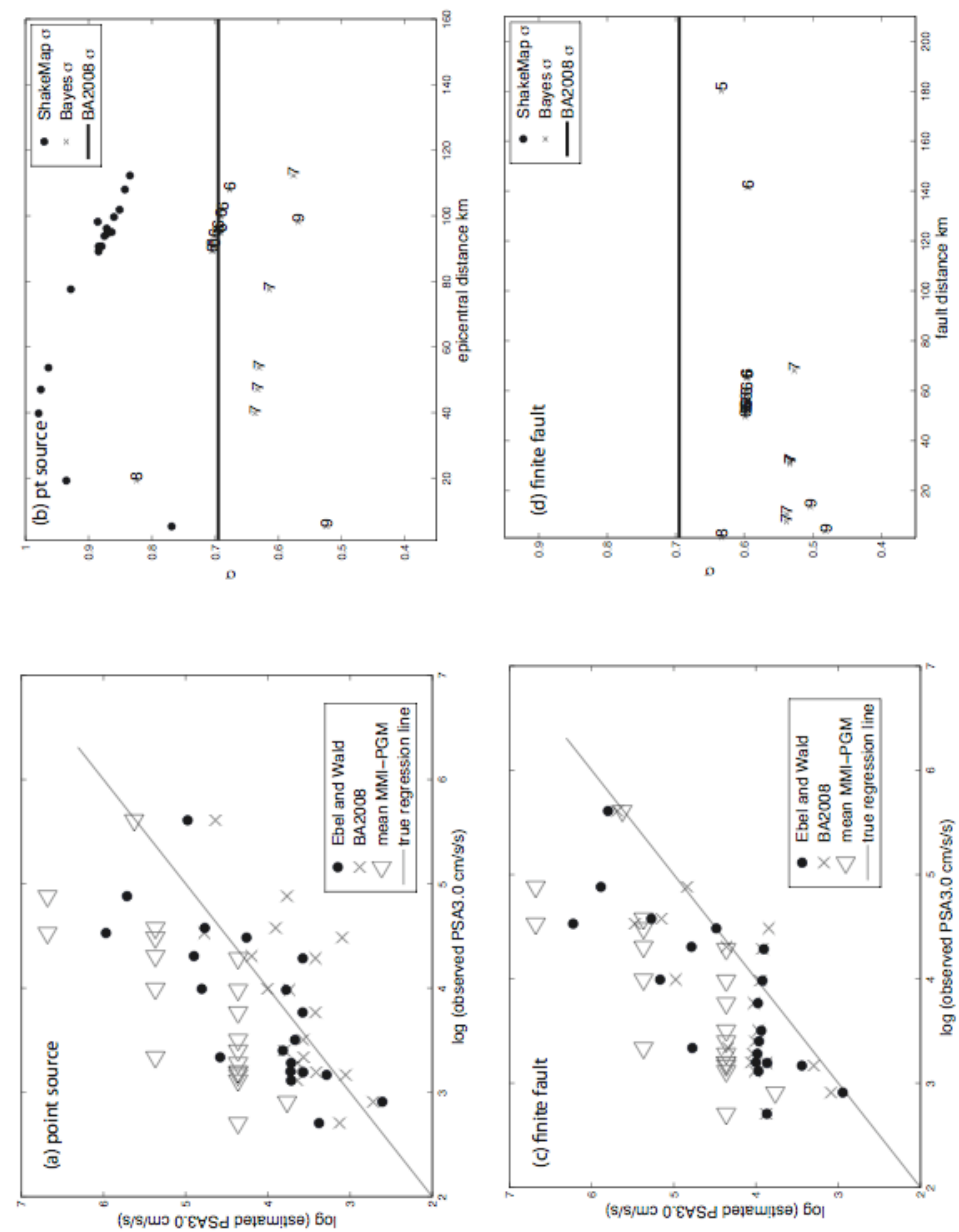

Figure 10: Kocaeli PSA 3.0 second period

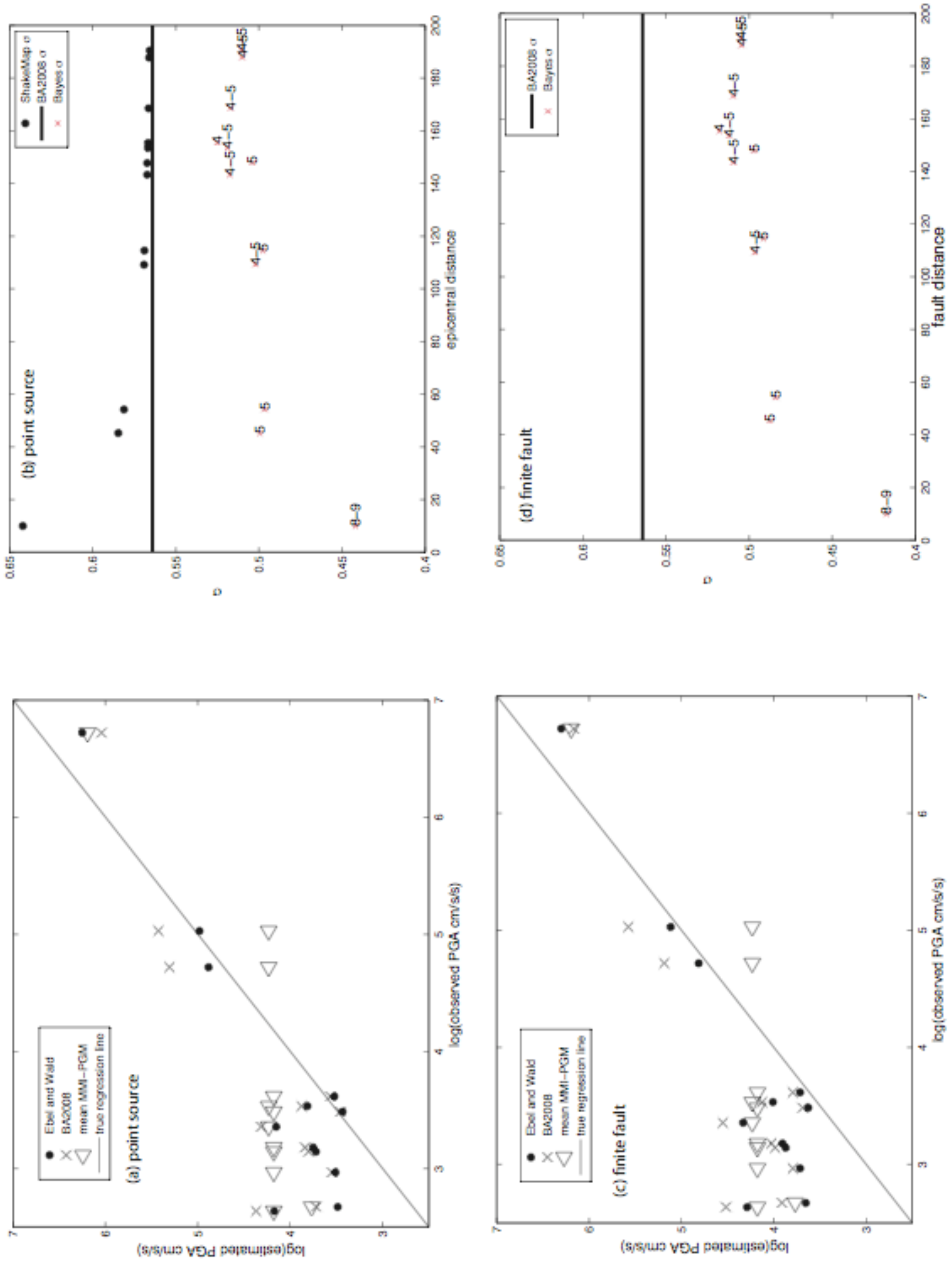

Figure 11: Bam PGA

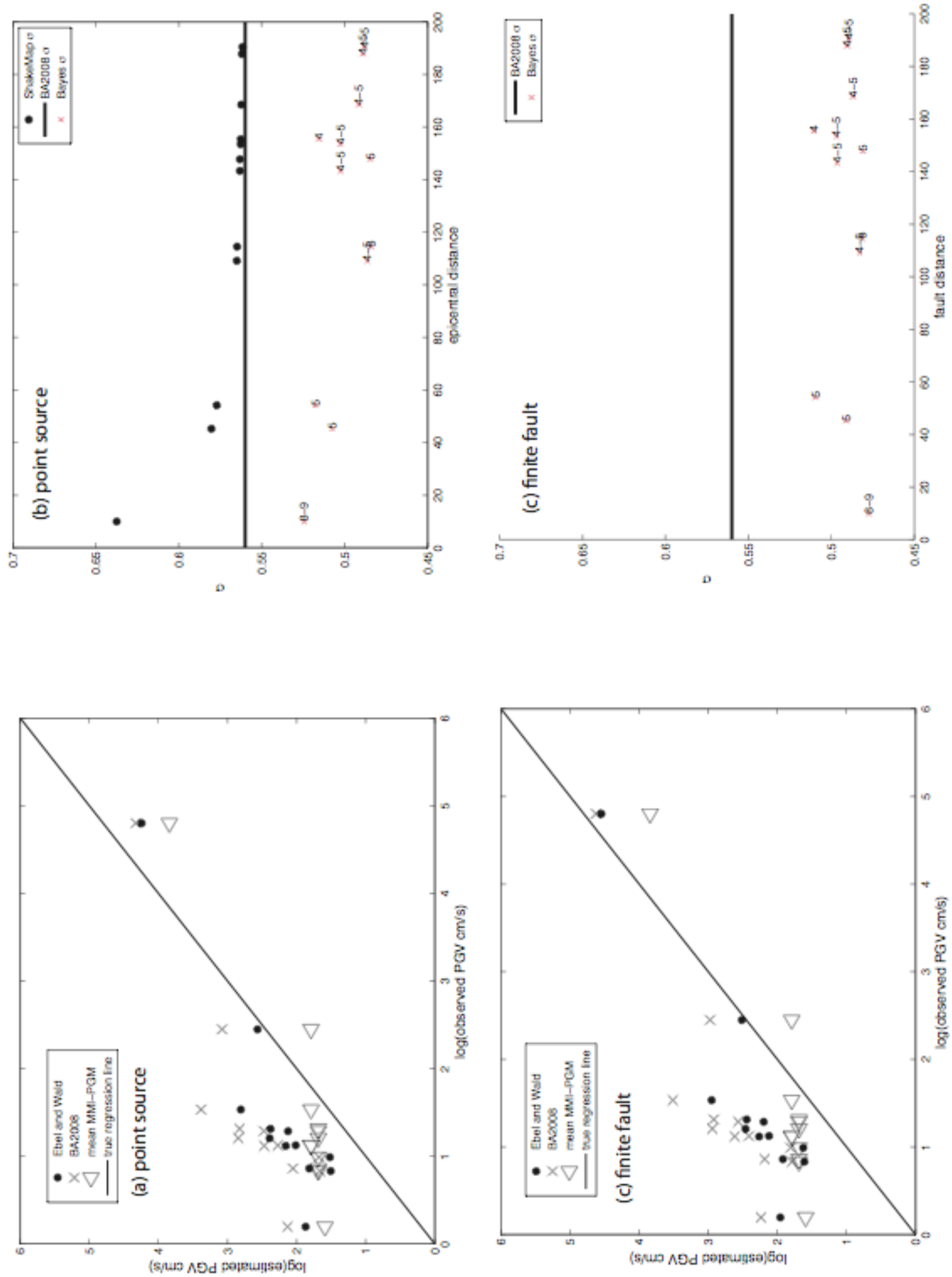

Figure 12: Bam PGV

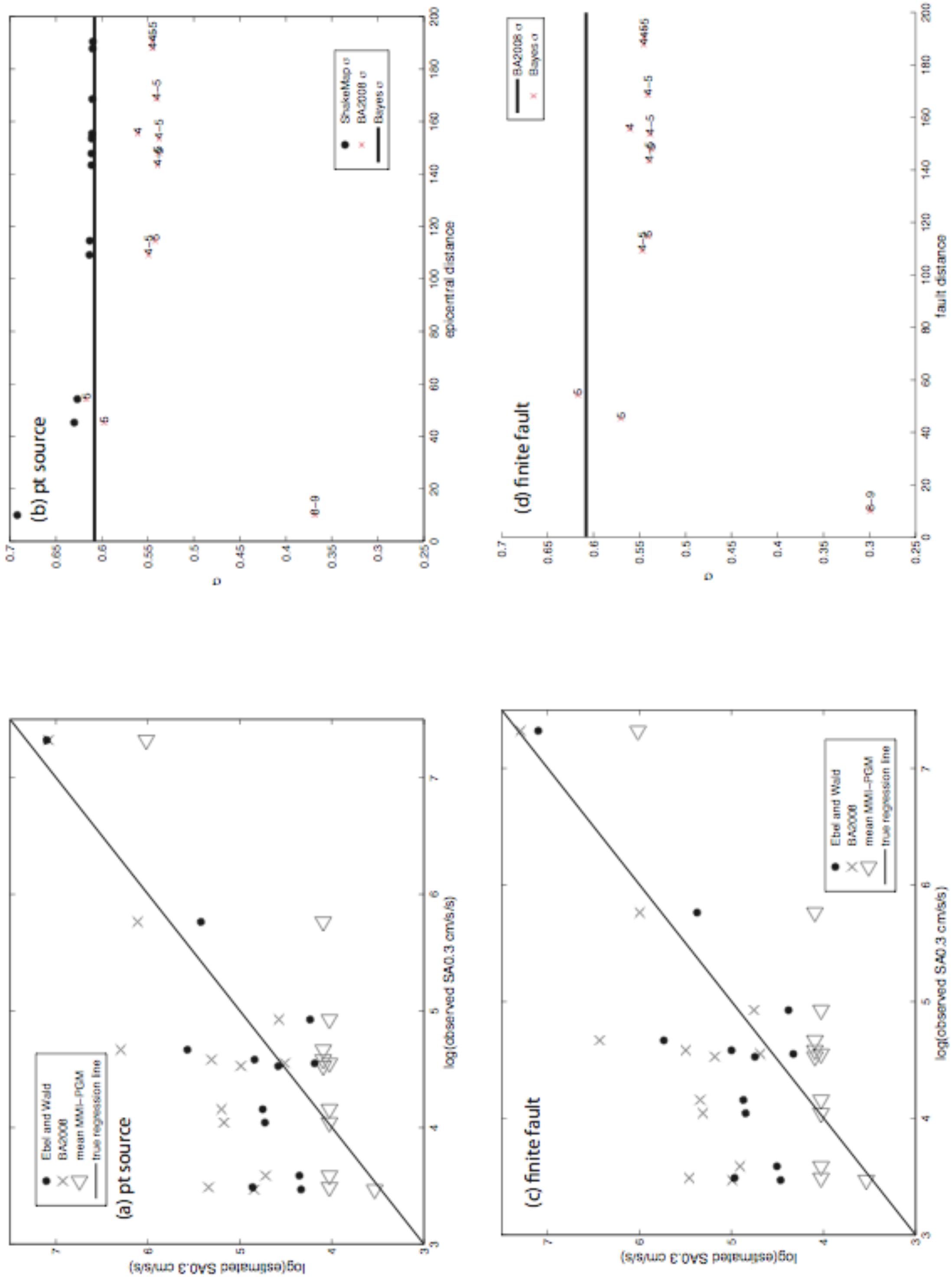

Figure 13: Bam PSA 0.3 second period

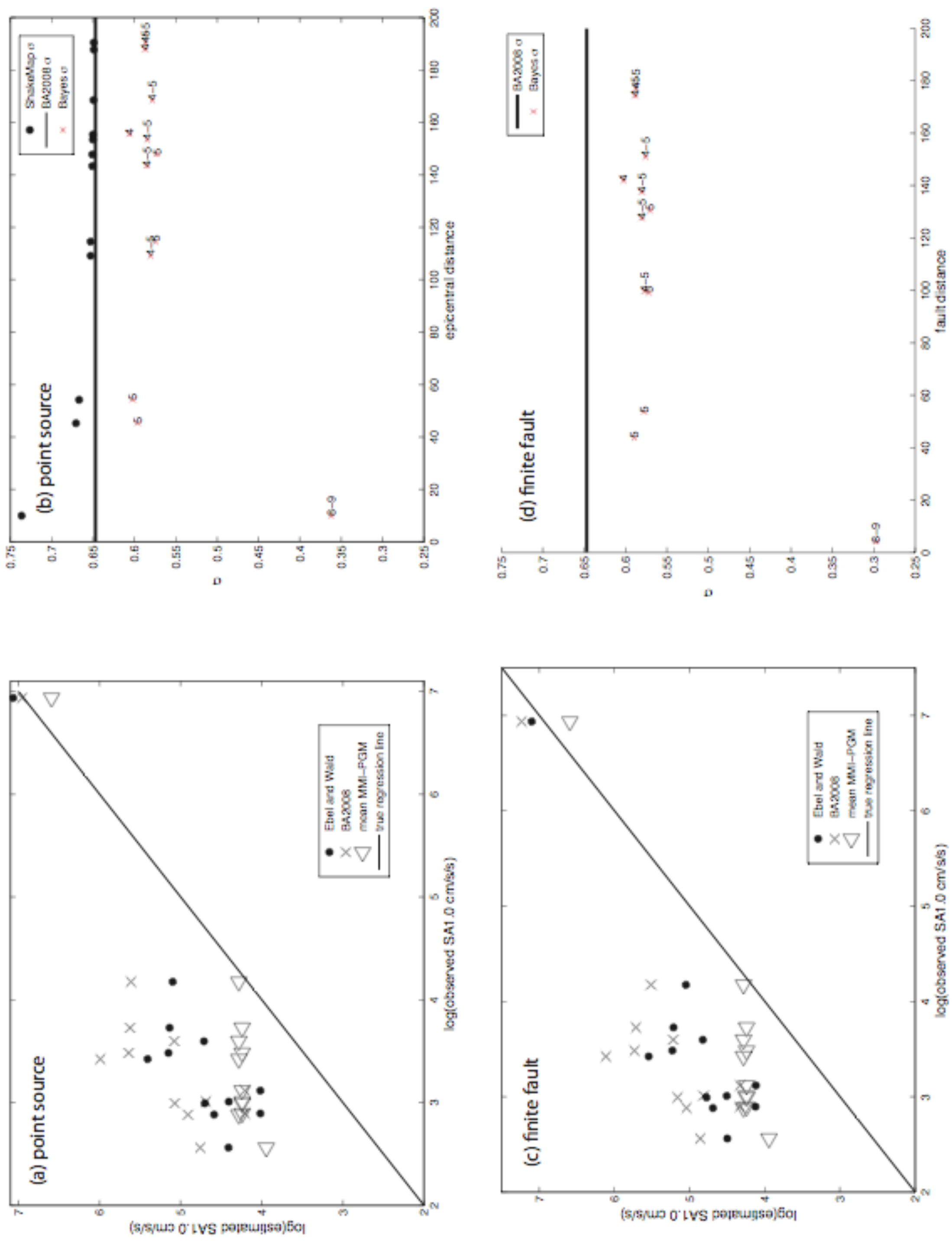

Figure 14: Bam PSA 1.0 second period

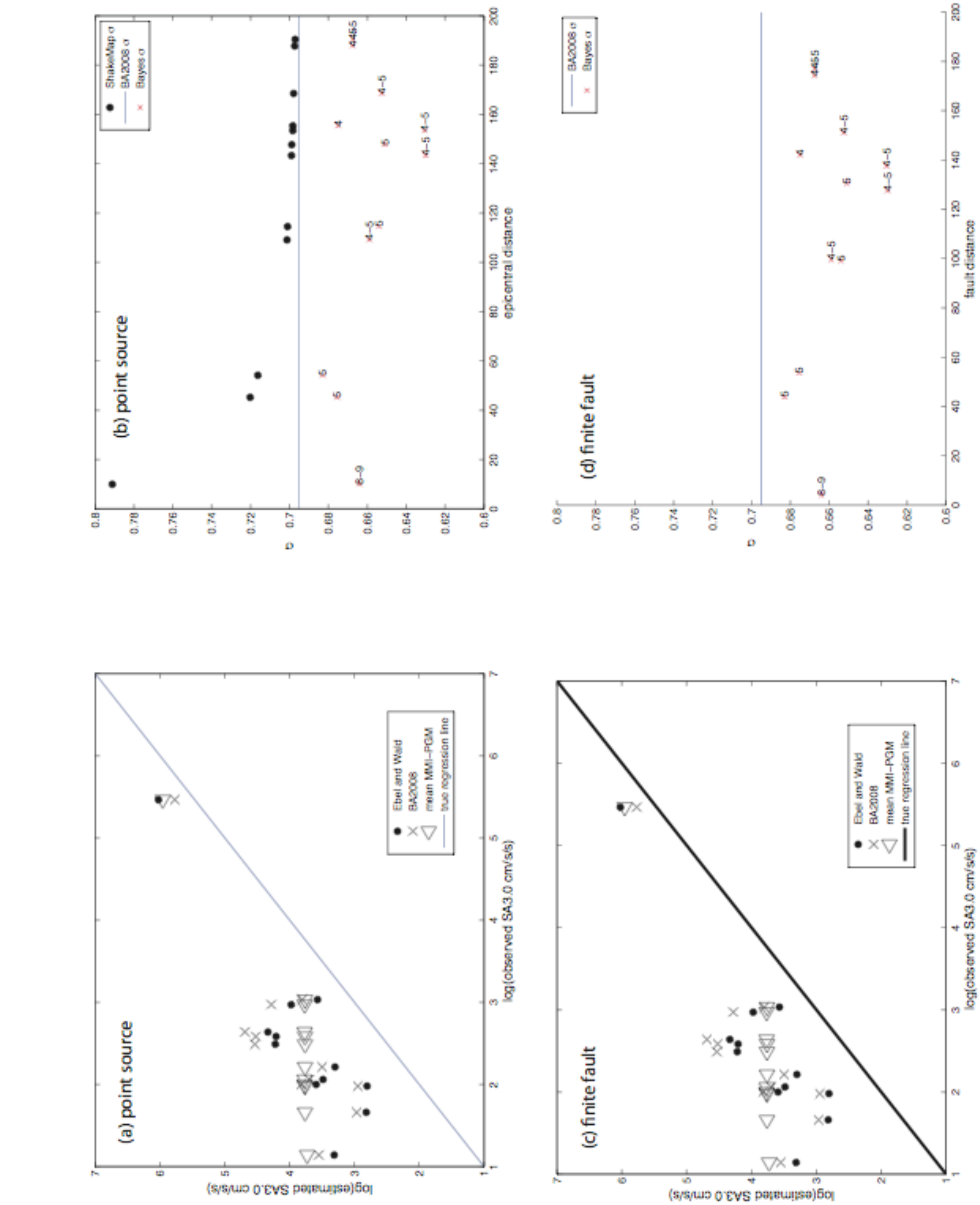

Figure 15: Bam PSA 3.0 second period

References

Atkinson, G. M., & Kaka, S. I. (2007). Relationships between Felt Intensity and Instrumental Ground Motion in the Central United States and California. *Bulletin of the Seismological Society of America, 97*(2), 497-510.

Atkinson, G. M., & Sonley, E. (2000). Empirical Relationships between Modified Mercalli Intensity and Response Spectra. *Bulletin of the Seismological Society of America, 90*(2), 537-544.

Boore, D., & Atkinson, G. (2008). Ground-motion prediction equations for the average horizontal component of PGA, PGV, and 5%-damped PSA at spectral periods between 0.01s and 10.0 s. *Earthquake Spectra, NGA Special Volume*.

Boore, D., Joyner, W. B., & Fumal, T. E. (1997). Equations for estimating horizontal response spectra and peak acceleration from western North American earthquakes: a summary of recent work. *Seismological Research Letters, 68*, 128-153.

Ebel, J., & Wald, D. (2003). Bayesian Estimations of Peak Ground Acceleration and 5% Damped Spectral Acceleration from Modified Mercalli Intensity Data. *Earthquake Spectra, 19*(3), 511-529.

http://www.bhrc.gov.ir/ISMN/index.htm. Iran Strong Motion Network.

Lin, K.-W., Wald, D., Worden, C. B., & Shakal, A. (2005). *Quantifying CISN ShakeMap uncertainty.* Paper presented at the California Geological Survey - SMIP05 Seminar.

Power, M., Chiou, B., Abrahamson, N., Bozorgnia, Y., Shantz, T., & Roblee, C. (2008). An overview of the NGA project. *Earthquake Spectra, NGA Special Volume*.

Sivia, D. S. (1996). *Data analysis: a Bayesian tutorial*: Oxford University Press.

Wald, D., Quitoriano, V., Heaton, T., Kanamori, H., Scrivner, C. W., & Worden, B. C. (1999a). TriNet "ShakeMaps": rapid generation of peak ground motion and intensity maps for earthquakes in southern California. *Earthquake Spectra, 15*(3), 537-556.

Wald, D., Quitoriano, V., Heaton, T. H., & Kanamori, H. (1999b). Relationships between Peak Ground Acceleration, Peak Ground Velocity, and Modified Mercalli Intensity in California. *Earthquake Spectra, 15*(3), 557-564.

Wald, D., Worden, B. C., Quitoriano, V., & Pankow, K. (2005). *ShakeMap Manual: Technical Manual, User's Guide, and Software Guide*: US Geological Survey.